Under frequency load shedding for low inertia grids utilizing smart loads

Article *in* International Journal of Electrical Power & Energy Systems · September 2021

DOI: 10.1016/j.ijepes.2021.107506

2 authors:

Amir Darbandsari
University of Tehran
5 PUBLICATIONS **8** CITATIONS
SEE PROFILE

Turaj Amraee
Khaje Nasir Toosi University of Technology
101 PUBLICATIONS **2,085** CITATIONS
SEE PROFILE

Electrical Power and Energy Systems 135 (2022) 107506

Contents lists available at ScienceDirect

International Journal of Electrical Power and Energy Systems

journal homepage: www.elsevier.com/locate/ijepes

Under frequency load shedding for low inertia grids utilizing smart loads

A. Darbandsari , T. Amraee *

Electrical Engineering Department, K. N. Toosi University of Technology, Tehran, Iran

ARTICLE INFO

Keywords:
Under frequency load shedding
Load duration curve
Low inertia
Renewables integration
Smart loads

ABSTRACT

Due to inertia deterioration which is caused by low inertia renewable resources, frequency-based protective schemes must be re-designed. This paper presents a multi-stage under frequency load shedding (UFLS) plan which is designed based on the yearly load duration curve (LDC) and activated according to the system frequency and the rate-of-change-of-frequency (RoCoF). In order to design a robust UFLS plan, a comprehensive list of credible operational and topological scenarios under different levels of renewables penetration are defined. For optimizing the UFLS performance over the constructed scenarios, a detailed system frequency response including the time response of governors, and natural load damping is developed. Then, the potential of frequency-dependent smart loads (SLs) as a remedy to postpone or reduce the total amount of load shedding in low inertia grids are investigated. Eventually, the proposed UFLS scheme is re-designed in the presence of SLs. The proposed method is formulated as a Mixed-Integer Linear Programming (MILP) model and solved using the CPLEX algorithm in GAMS and the effectiveness of the proposed method is investigated for the dynamic IEEE 39-bus test system.

1. Introduction

1.1. Motivations and background

Nowadays, due to economic and environmental concerns, the use of renewable energy resources has increased significantly. The integration of non-synchronous renewable resources comes up with some negative impacts on system operation and stability [1]. In addition to the operational challenges caused by the intermittency of renewable resources, the frequency stability is highly affected by inertia deterioration [2]. Taking a glance at reports of 9th august 2019 UK blackout is the evidence of this issue [3]. Therefore, as the penetration of renewable resources increases, the UFLS plans must be modified to guarantee the frequency stability during severe generation deficiencies [4].

UFLS schemes are categorized as multi-stage, semi-adaptive and adaptive schemes. In multistage UFLS, as most common used scheme in practice, the protective relays are set offline to shed predetermined percentage of load during a few stages when the frequency falls below a given threshold during a time delay [5]. In [6], the details of the multistage UFLS in different utilities around the world have been presented. Additionally, different kinds of uncertainties can be assumed in UFLS design. Authors in [7] have proposed a probabilistic UFLS scheme in which the uncertainties of generation deficiency, inertia time constant and load damping factor are handled using Monte-Carlo method. In semi-adaptive UFLS, the load shedding is activated based on the frequency magnitude and RoCoF value. Using RoCoF values, the semi-adaptive schemes adjust their responses based on the amount of generation deficiency or contingency severity [8].

In adaptive UFLS, the load shedding is carried out, totally, according to the RoCoF values. Using wide area monitoring systems (WAMS) and phasor measurement units (PMUs), the implementation of adaptive UFLS schemes is realized [9]. Using PMU data, in adaptive UFLS the frequency and voltage stability can be improved, simultaneously [10]. Due to oscillatory variations of RoCoF value, the use of pure adaptive UFLS plan scheme is not very common in practice.

Due to simplicity, the application of Multi-stage UFLS scheme is more common. But, the greater the penetration of renewable resources the more resilient UFLS schemes are required. Therefore, using adaptive UFLS schemes in future networks with high penetration of inertia-free resources is inevitable.

Authors in [11] have used Genetic Algorithm for UFLS design. The effects of renewables integration in UFLS design have been addressed in [12,13]. In [12], the authors present a novel UFLS scheme for a microgrid consisting of synchronous and non-synchronous units. In [13], authors propose a UFLS design using polynomial neural network (PNN). In [14] a novel method is proposed for determining the required load shed and time delay at each stage of UFLS for an offshore

* Corresponding author.
E-mail address: amraee@kntu.ac.ir (T. Amraee).

https://doi.org/10.1016/j.ijepes.2021.107506
Received 20 April 2021; Received in revised form 22 June 2021; Accepted 10 August 2021
Available online 15 September 2021

Nomenclature

Indices

n	Index of time steps
m	Index of smart loads
s	Index of load shedding stages
c	Index of contingencies
i	Index of generators

Parameters

H_i/H_{eq}	Inertia time constant of i^{th} generator/Equivalent inertia of the network
D	Load damping factor
S_i/S	Apparent power of i^{th} generator/base apparent power of the system
R_i/R_{eq}	Governor droop of i^{th} generator/equivalent governor droop of the network
N	Total number of time steps for simulation
N_g	Number of generators
N_s	Number of load shedding stages
N_{SL}	Number of smart loads
f_0	Nominal frequency of the system
T_g	The time constant of governor
T_s	The time constant of smart load
L	Arbitrary large positive number
Δt_s	Time delay of UFLS plan
f_{min}/f_{max}	Minimum/maximum allowable frequency of the network
Δf_{ss}^{min}	Minimum allowable deviation of steady state frequency
Δf_{ss}^{max}	Maximum allowable deviation of steady state frequency
ΔP_s^{min}	Minimum allowable load shedding at each stage
ΔP_s^{max}	Maximum allowable load shedding at each stage
ΔP_{max}^{shed}	Total amount of allowable load shedding
Δt	Time step in discretized frequency response
$kpf-m$	Frequency-sensitivity of smart load type$m$
$kpv-m$	Voltage-sensitivity of smart load type$m$
f_m^{dr-min}	Minimum allowable operating drive frequency of smart load typem^{th}
f_m^{dr}	Drive frequency of smart load type$m$

Variables

ΔP^c	Amount of generation outage at each event
$\Delta P_{n,c}^{gov}$	Power change by governor at n^{th} time step and under c^{th} contingency
$\Delta f_{n,c}$	Frequency deviation of the system at n^{th} time step and under c^{th} contingency
f_s	Frequency threshold at each load shedding stage
Δf_{ss}	Steady state deviation of the frequency
ΔP_s^{shed}	The amount of load shedding at each stage
$u_{s,n}^c$	Auxiliary binary variable for load shedding of stage s n^{th} time step and under c^{th} contingency
$V_{s,n}^c$	Auxiliary binary variable of delay timer for load shedding of stage s
$\Delta t_{s,n}^c$	Time delay before load shedding of stage s^{th} at n^{th} time step and under c^{th} event
$x_{s,n,c}$	Auxiliary variable utilized for linearization
$B_{s,n,c}$	Auxiliary variable utilized for linearization
Res_m^{max}	Maximum amount of reserve provided by smart load type m
$\Delta P_{n,m}^{SL}$	Load reduction by smart load type m at time step n

standalone power system near Taiwan and the optimization model is solved by PSO algorithm. A new continuous UFLS plan is proposed by authors in [15] which is analyzed with a closed-form solution of frequency dynamics. The main merit about this method is to implement the continuous scheme for systems without continuously controllable loads.

Beside UFLS schemes for frequency restoration, there are some auxiliary services which can be used in primary frequency control. In [16] a simplified model has been proposed for DFIG-based wind turbines using a virtual inertia controller which works based on optimized power point tracking (OPPT) method. Results show that using the proposed method, wind farms will be able to contribute in primary frequency control and to reduce frequency fluctuations. Additionally, authors in [17] have shown that utilizing fast-acting energy storages by acting as a synthetic inertia can mitigate the impact of renewable energy resources in an islanded grid in the case of generation outages Authors in [18] have proposed a predictive UFLS which predicts nadir frequency following an outage. Then, it predicts the available ancillary services (i.e. fast spinning reserve, energy storage systems and so on) in order to eliminate the unnecessary load shedding. Recently, the potential of smart loads in the primary frequency control has been considered. Smart loads are typical loads that can participate in frequency support using certain power-electronic devices [19]. In [20], authors have considered both thermo-static smart load and the electric dynamic smart load (i.e. the refrigerator) in primary frequency control to achieve lower amount of load shedding. As a major research gap in previous proposed UFLS schemes, the proposed plans are set for a base case operating point and no effort has been done to design the UFLS plan according to the credible scheduling of generating units during a given year. In fact, the performance of the UFLS plan highly depends on the equivalent inertia of committed units at possible loading conditions. Also, the potential of smart load in reducing or postponing the load shedding has not been addressed in low inertia or non-synchronous-penetrated networks.

1.2. Contributions

In this paper, a RoCoF-based multi-stage UFLS plan is proposed. The major contributions of this paper are summarized as follows:

1. Proposing a UFLS plan with considering a comprehensive list of credible unit scheduling using an MIP model of unit commitment over a yearly LDC which at each load point based on the committed units and loading condition, the credible generation outages and contingencies are considered.
2. Optimizing the UFLS plan via an MIP optimization model considering the system frequency response. Governor actions, natural load damping, generation outage, and load shedding are all included in the discretized system frequency response.
3. Modeling smart load contribution in primary frequency control to reduce the amount of load shedding or postpone the activation of UFLS plan. In fact, the UFLS plan is modified in presence of smart loads and high penetration of non-synchronous renewables.

1.3. Paper organization

The rest of this paper is organized as follows. Overall structure of the proposed method is presented in Section 2. The proposed UFLS method with discretized system frequency response considering Smart Load is formulated in Section 3. The proposed procedure for scenario construction based on the unit commitment study and outage scenarios is given in Section 4. The simulation results are discussed in Section 5.

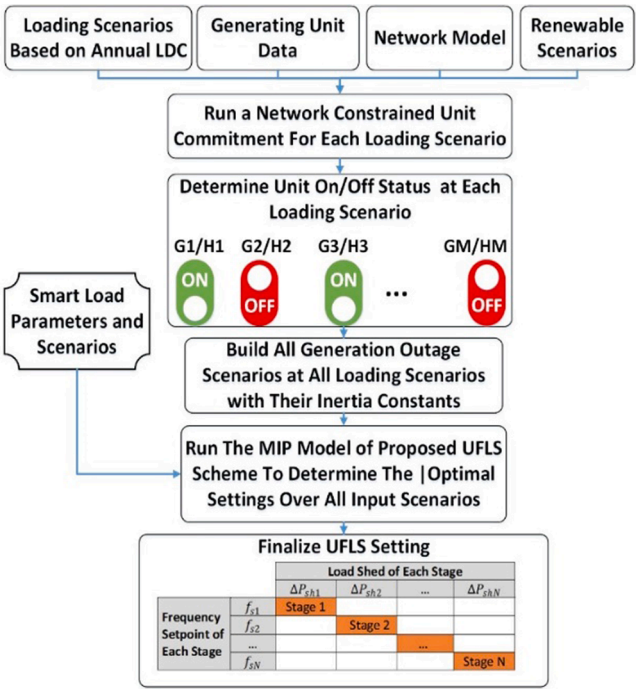

Fig. 1. Overall structure of the proposed method.

Finally, the paper is concluded in Section 6.

2. Overall structure of the proposed method

Overall structure of the proposed method is shown in Fig. 1. In previous proposed schemes, the UFLS plan is optimized at a base-case scenario such as peak load condition and the outage scenarios are formed around this base case point. However, the frequency stability highly depends on the equivalent inertia or set of committed synchronous units and in some cases, such as light load conditions, the frequency stability may be more critical due to the lack of committed synchronous units.

According to yearly LDC, the loading conditions vary from time to time all over the year. Each loading condition has its own set of committed generating units. However, the UFLS plan has a unique setting that must be optimized over all credible scenarios. To this end, in this paper, based on a standard LDC, at each loading point a Unit Commitment (UC) study is carried out and the set of committed generating units are determined. The amount of equivalent inertia constant is then determined for each UC scheduling plan. As the penetration of renewable increases, the frequency support will be more critical. Worst case scenarios happen when the penetration of renewable generation is high and just a few number of synchronous generators are committed [2]. A suitable UFLS scheme must support the network frequency all the time and under whole credible loading conditions and outage scenarios.

3. Formulation of the proposed method

3.1. System frequency response

The system frequency response can be represented as given in (1) using the continuous swing equation [5]. The activation of governors and load damping are integrated into the swing equation. The swing equation and dynamic response of governor are considered as given in (1) and (2), respectively.

$$\frac{d\Delta f(t)}{dt} = (1/2H_{eq})(\Delta P^{gov}(t) - \Delta P^{c} - D\Delta f(t)) \tag{1}$$

$$\frac{d\Delta P^{gov}(t)}{dt} = \frac{1}{T_g}(-\Delta P^{gov}(t) - \frac{\Delta f(t)}{R_{eq}}) \tag{2}$$

In order to obtain the system frequency response on COI, the equivalent inertia of the network and the equivalent governors' droop are calculated using (3) and (4) respectively.

$$H_{eq} = \sum_{i=1}^{N_g}(H_i S_i)/S \tag{3}$$

$$R_{eq} = \sum_{i=1}^{N_g}(R_i S)/S_i \tag{4}$$

The frequency response and the dynamic of governor is discretized using (5) and (6) into time step ofΔt.

$$\Delta f(n\Delta t) = \Delta f_n \tag{5}$$

$$\Delta P^{gov}(n\Delta t) = \Delta P_n^{gov} \tag{6}$$

After discretization using (5) and (6), the frequency response and governor dynamic are rewritten respectively as follows:

$$\Delta f_{n+1} = \Delta f_n + \int_{t_n}^{t_{n+1}} \frac{1}{2H_{eq}}\left(\Delta P_n^{gov} - \Delta P^{c} - D\Delta f_n\right) \tag{7}$$

$$\Delta P_{n+1}^{gov} = \Delta P_n^{gov} + \frac{\Delta t}{T_g}\left(\frac{-\Delta f_{n+1}}{R_{eq}} - \Delta P_n^{gov}\right) \tag{8}$$

According to (9) and based on the trapezoidal rule, the discretized response given in (7) can be approximated as (10):

$$K_n = \frac{1}{H_{eq}}\left(\Delta P_n^{gov} - \Delta P^{c} - D\Delta f_n\right) \tag{9}$$

$$\Delta f_{n+1} \simeq \Delta f_n + \frac{\Delta t}{2}[K_n(t_n, \Delta f_n) + K_n(t_{n+1}, \Delta f_{n+1})] \tag{10}$$

3.2. UFLS formulation

In this section, the mathematical model of the proposed multi-stage UFLS plan is presented. UFLS plan is set to shed a predetermined percentage of load when the frequency remains below a certain frequency thresholds for a given time delay. Therefore, every relay needs a timer to calculate the time, when the system frequency drops below the frequency set-points of the UFLS plan. The constraints given in (11)–(13) are introduced to model the relay's timer.

$$\frac{f_s - (f_0 + \Delta f_n^c)}{L} \le V_{s,n}^c \le 1 + \frac{f_s - (f_0 + \Delta f_n^c)}{L}, \forall c, s, n \tag{11}$$

$$\Delta t_{s,n}^c = \Delta t_{s,n-1}^c + V_{s,n}^c \Delta t, \forall c, s, n \tag{12}$$

$$\frac{\Delta t_{s,n}^c - \Delta t_s}{L} \le u_{s,n}^c \le 1 + \frac{\Delta t_{s,n}^c - \Delta t_s}{L}, \forall c, s, n \tag{13}$$

Considering the activation of UFLS plan the discretized swing equation is modified as follows:

$$K_n = \frac{1}{H_{eq}}\left(\Delta P_{n,c}^{gov} - \Delta P^{c} - D\Delta f_{n,c} + \sum_{s}^{N_s} u_{s,n}^c \Delta P_s^{shed}\right) \tag{14}$$

To develop an MIP model, using auxiliary constraints in (15)–(19), the nonlinear term of $u_{s,n}^c \Delta P_s^{shed}$ is linearized.

$$x_{s,n,c} = u_{s,n}^c \Delta P_s^{shed} \tag{15}$$

$$\Delta P_s^{shed} - x_{s,n,c} \ge 0 \tag{16}$$

$$\Delta P_s^{shed} - x_{s,n,c} \le (1 - u_{s,n}^c) \tag{17}$$

$$x_{s,n,c} \le u_{s,n}^c \tag{18}$$

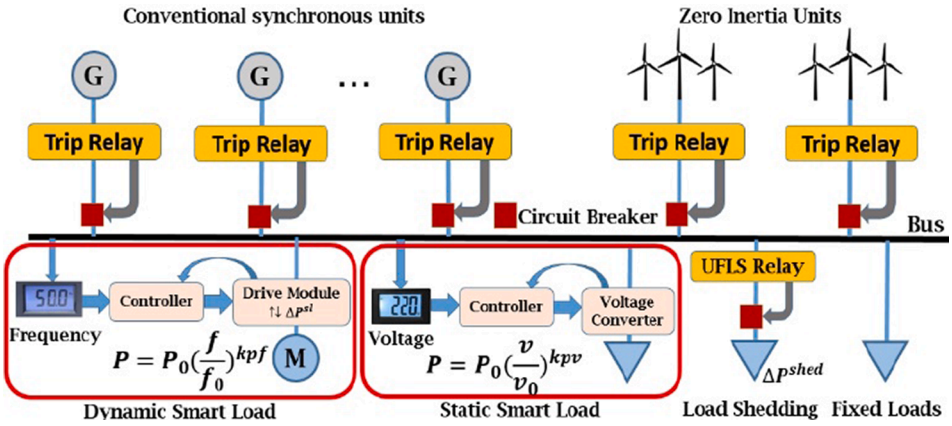

Fig. 2. Conceptual schematic of smart loads and their operation.

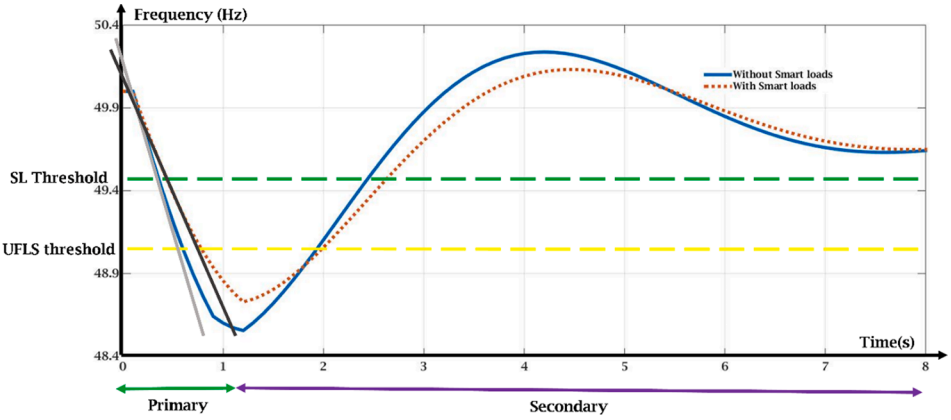

Fig. 3. Effects of SLs on frequency response.

$$x_{s,n,c} \geq 0 \tag{19}$$

Some practical limits are needed to be imposed on frequency nadir (i.e. the minimum point of frequency response), steady state frequency, and the amount of load shed in each stage. According to (20), the frequency response at each time instant must remain inside a predetermined safe zone. The steady state deviation of the system frequency is constrained as given in (21). The amount of load shedding at each stage and the total amount of load shedding are limited according to (22) and (23), respectively. A major setting of the multistage UFLS plan is the frequency set point that is bounded using (24). According to the constraint given in (25), the load shedding at each stage is not allowed to be restored during the simulation. To avoid the simultaneous activation of UFLS stages, the constraints given in (26) and (27) are defined. Finally, to prevent any conflict between subsequent stages, a given interval is defined between two subsequent frequency set points as given in (28).

$$f_{min} \leq f_{n,c} = f_0 + f_0 \Delta f_{n,c} \leq f_{max} \tag{20}$$

$$\Delta f_{ss}^{min} \leq \Delta f_{ss} \leq \Delta f_{ss}^{max} \tag{21}$$

$$\Delta P_s^{min} \leq \Delta P_s^{shed} \leq \Delta P_s^{max} \tag{22}$$

$$\sum_{s}^{N_s} \Delta P_s^{shed} \leq \Delta P_{max}^{shed} \tag{23}$$

$$f_s^{max} \leq f_s \leq f_s^{min} \tag{24}$$

$$u_{s,n}^{c} \geq u_{s+1,n}^{c} \tag{25}$$

$$\sum_{s}^{N_s} u_{s,n}^{c} - \sum_{s}^{N_s} u_{s,n-1}^{c} \leq 1 \tag{26}$$

$$u_{s,n}^{c} \geq u_{s,n-1}^{c} \tag{27}$$

$$f_s - f_{s+1} \geq 0.2 \tag{28}$$

The objective function of the proposed UFLS is defined to minimize the total amount of load to be shed as follows:

$$OF = \min \sum_{c} \sum_{s=1}^{N_s} x_{s,N,c} \tag{29}$$

Different kinds of UFLS plans can be designed (e.g. Equal Block, Decreasing and Increasing scheme). In Equal Block UFLS plan, the amount of load shed in all stages are equal, while in a Decreasing scheme more load is shed in early stages. In low inertia power systems, under a significant generation outage, the frequency and its RoCoF change sharply. In such situations, a Decreasing UFLS plan is more suitable because it can shed almost large amount of load at initial stages [21]. However, the amount of load shedding at each stage and frequency thresholds must be optimized. In conventional network with low penetration of non-synchronous resources, the Increasing UFLS plans are preferred [21]. Since in Decreasing UFLS plans, the larger amount of load is shed at early stages, the following constraint is introduced and added to the MIP model of the UFLS plan:

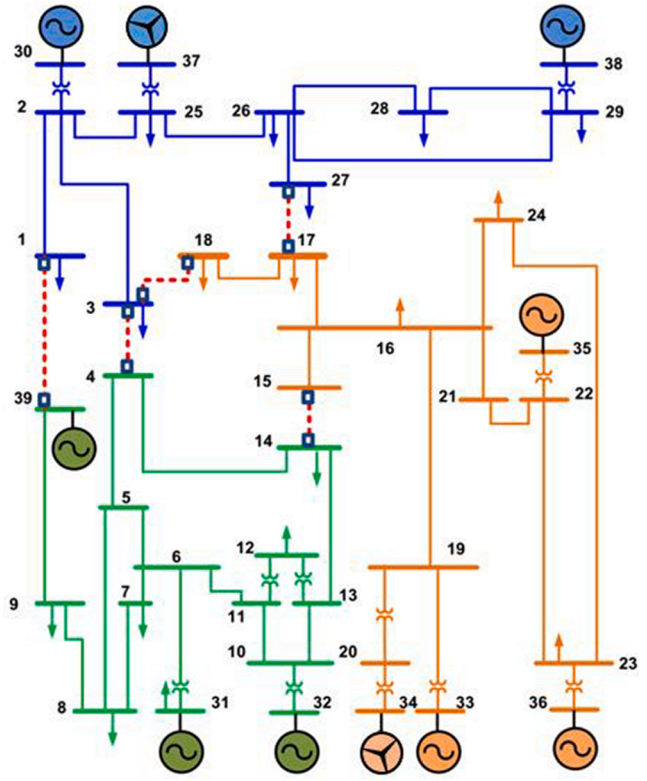

Fig. 4. Single line diagram of IEEE 39 bus system.

$$\Delta P_{s+1}^{shed} * u_{s+1,n}^{c} \le \Delta P_{s}^{shed} * u_{s+1,n}^{c} - 0.01 * u_{s+1,n}^{c} \tag{30}$$

The nonlinear term of $\Delta P_{s}^{shed} * u_{s+1,n}^{c}$ is linearized via the auxiliary constraints given in (31)–(35).

$$B_{s,n,c} = \Delta P_{s}^{shed} * u_{s+1,n}^{c} \tag{31}$$

$$B_{s,n,c} \le \Delta P_{s}^{shed} \tag{32}$$

$$B_{s,n,c} \ge \Delta P_{s}^{shed} - (1 - u_{s+1,n}^{c}) \tag{33}$$

$$B_{s,n,c} \ge 0 \tag{34}$$

$$B_{s,n,c} \le u_{s+1,n}^{c} \tag{35}$$

A similar procedure can be persuaded for Increasing UFLS. It should be noted that the UFLS scheme is only designed for non-critical loads and the priority of non-critical loads has been considered the same during the UFLS optimization. However, by assigning a weight factor to each load point, the related load points are prioritized. This weight factor represents the cost of load shedding at each load point.

3.3. Smart load contribution in frequency support

SLs are typical non critical loads which due to using power electronic interfaces, they will be able to control their power consumption and participate in primary frequency control [16]. In general, SLs are divided into static and dynamic SLs as shown in Fig. 2. The consumption of static SLs (e.g. lighting loads, and water heating) heavily depends on the input voltage magnitude and by using a voltage converter and some auxiliary power electronic devices, their consumptions can be controlled [16].

On the other hand, the consumption of dynamic rotating loads like industrial motors heavily depends on the input frequency [22]. So by utilizing a drive system (which they mostly have) and by making small changes in its circuit, they will be able to decrease their consumptions under frequency deviation caused by generation outage in main grid [16]. The amount of short term reserve that every smart load can prepare depends on its dependency to input voltage or frequency [16]. Also, according to capability curves, electrical and mechanical limitations are very important to determine how long the short term reserve can be delivered [16]. Regarding these issues, it seems using dynamic smart loads require less investment cost, while static smart loads need some power electronic devices (i.e. convertors) in order to adjust their input voltage. In this paper, only dynamic smart loads are taken into account for frequency support.

According to above discussion, SLs are used in primary frequency control to postpone or reduce the amount of required load shedding. As shown in Fig. 3, SLs activation threshold is earlier than UFLS action and affects the frequency response both by reducing the ROCOF and improving the nadir frequency.

The amount of reserve that a dynamic smart load can deliver to the network is determined as follows [16]:

$$Res_{m}^{max} = P_{0-i,m}\left[\left(\frac{f_{m}^{dr}}{f_{0}}\right)^{kpf-m} - \left(\frac{f_{m}^{dr-min}}{f_{0}}\right)^{kpf-m}\right] \tag{36}$$

The response of a smart load is discretized as follows [23]:

$$\Delta P_{n,m}^{SL} = \Delta P_{n-1,m}^{SL} + \frac{\Delta t}{T_{s}}\left(Res_{m}^{max} - \Delta P_{n-1,m}^{SL}\right) \tag{37}$$

By integrating the dynamic smart loads into the UFLS model, th-e system frequency response is modified as follow:

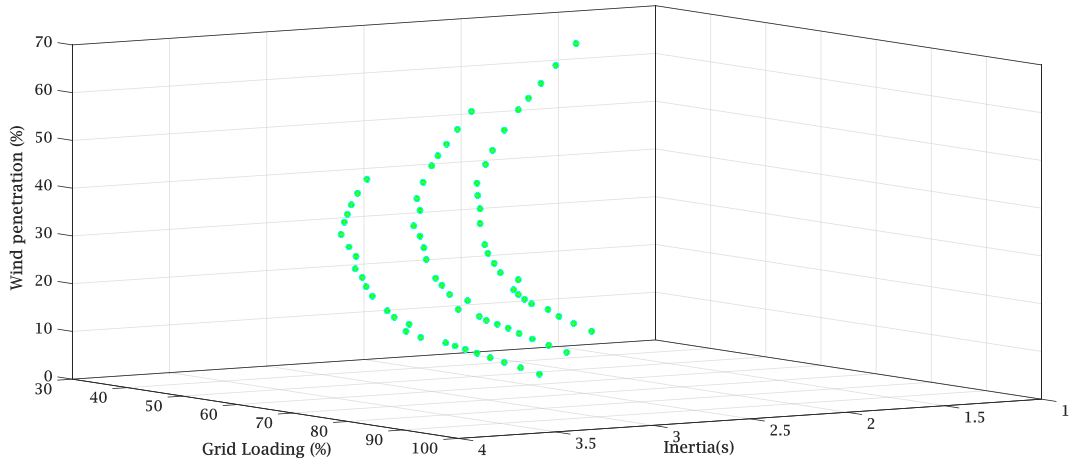

Fig. 5. 75 credible loading scenarios under 3 levels of wind generation and annual LDC.

Table 1
Annual unit commitment results.

Load factor (%)		**100**	**95**	**92**	**89**	**86**	**84**	**82**	**80**	**77**	**74**	**71**	**68**	**65**	**59**	**56**	**53**	**50**	**47**	**44**	**41**	**39**	**37**	**36**	**34**	**32**
Load Point		**1**	**2**	**3**	**4**	**5**	**6**	**7**	**8**	**9**	**10**	**11**	**12**	**13**	**14**	**15**	**16**	**17**	**18**	**19**	**20**	**21**	**22**	**23**	**24**	**25**
Gen. numbers	30	1	1	1	1	1	1	1	1	1	1	1	1	1	1	1	1	1	1	1	1	1	1	1	1	1
	31	1	1	1	1	1	1	1	1	1	1	1	1	1	1	1	1	1	1	1	1	1	1	1	1	1
	32	1	1	1	1	1	1	1	1	1	1	1	1	1	1	1	1	1	0	0	0	0	0	0	0	0
	33	1	1	1	1	1	1	1	1	1	1	1	1	1	1	1	1	1	1	1	1	1	1	1	1	1
	34	1	1	1	1	1	1	1	1	1	1	1	1	1	1	1	1	1	1	1	1	1	1	1	1	1
	35	1	1	1	1	1	1	1	1	1	1	1	1	1	0	0	0	0	0	0	0	0	0	0	0	0
	36	1	1	1	1	1	0	0	0	1	0	1	0	0	0	0	0	0	0	0	0	0	0	0	0	0
	37	1	1	1	1	1	1	1	1	1	1	1	1	1	1	1	1	1	1	1	1	1	1	1	1	1
	38	1	1	1	1	1	1	1	1	0	0	0	0	0	0	0	0	0	0	0	0	0	0	0	0	0
	39	1	1	1	1	1	1	1	1	1	1	0	0	0	0	0	0	0	0	0	0	0	0	0	0	0
Load Point		**26**	**27**	**28**	**29**	**30**	**31**	**32**	**33**	**34**	**35**	**36**	**37**	**38**	**39**	**40**	**41**	**42**	**43**	**44**	**45**	**46**	**47**	**48**	**49**	**50**
Gen. numbers	30	1	1	1	1	1	1	1	1	1	1	1	1	1	1	1	1	1	1	1	1	1	1	1	1	1
	31	1	1	1	1	1	1	1	1	1	1	1	1	1	1	1	1	1	1	1	1	1	1	1	1	1
	32	1	1	1	1	1	1	1	1	1	1	1	1	1	1	1	1	1	0	0	0	0	0	0	0	0
	33	1	1	1	1	1	1	1	1	1	1	1	1	1	1	1	1	1	1	1	1	1	1	1	1	1
	34	1	1	1	1	1	1	1	1	1	1	1	1	1	1	1	1	1	1	1	1	1	1	1	1	1
	35	1	1	1	1	1	1	1	1	1	1	1	1	1	0	0	0	0	0	0	0	0	0	0	0	0
	36	1	1	1	1	1	0	0	0	0	0	0	0	0	0	0	0	0	0	0	0	0	0	0	0	0
	37	1	1	1	1	1	1	1	1	1	1	1	1	1	1	1	1	1	1	1	1	1	1	1	1	1
	38	1	1	1	1	1	1	1	1	0	1	0	0	0	0	0	0	0	0	0	0	0	0	0	0	0
	39	1	1	1	1	1	1	1	1	1	0	0	0	0	0	0	0	0	0	0	0	0	0	0	0	0
Load Point		**51**	**52**	**53**	**54**	**55**	**56**	**57**	**58**	**59**	**60**	**61**	**62**	**63**	**64**	**65**	**66**	**67**	**68**	**69**	**70**	**71**	**72**	**73**	**74**	**75**
Gen. numbers	30	1	1	1	1	1	1	1	1	1	1	1	1	1	1	1	1	1	1	1	1	1	1	1	1	1
	31	1	1	1	1	1	1	1	1	1	1	1	1	1	1	1	1	1	1	1	1	1	1	1	1	1
	32	1	1	1	1	1	1	1	1	1	1	1	1	1	1	1	1	1	0	0	0	0	0	0	0	0
	33	1	1	1	1	1	1	1	1	1	1	1	1	1	1	1	1	1	1	1	1	1	1	1	1	1
	34	1	1	1	1	1	1	1	1	1	1	1	1	1	1	1	1	1	1	1	1	1	1	1	1	1
	35	1	1	1	1	1	1	1	1	1	1	1	0	0	0	0	0	0	0	0	0	0	0	0	0	0
	36	1	1	1	1	1	1	1	1	0	0	0	0	0	0	0	0	0	0	0	0	0	0	0	0	0
	37	1	1	1	1	1	1	1	1	1	1	1	1	1	1	1	1	1	1	1	1	1	1	1	1	1
	38	1	1	1	1	0	0	0	0	0	0	0	0	0	0	0	0	0	0	0	0	0	0	0	0	0
	39	1	1	1	1	1	1	1	1	0	0	0	0	0	0	0	0	0	0	0	0	0	0	0	0	0

Table 2
Outage credible scenarios.

Scenario Type	Gen.	WF	Isolating lines
Single Outages	30–39	34,37	–
Double Outages	30–39	34,37	–
North Island	30,37,38	37	(1–39),(3–18), (17–27)
East Island	33,34,35,36	34	(3–18),(17–27), (14–15)
West Island	31,32,39	–	(1–39),(3–4), (14–15)
Maximum single and double outage in each island	30–39	34,37	–

Table 3
Input parameters for simulation.

Simulation Parameters	Value
D	1.5 p.u.
R_{eq}	0.1 p.u.
f_0	50 Hz
T_g	10 s
L	1000
f_{imn}/f_{max}	47.5/50.5 Hz
$\Delta f_{ss}^{min}/\Delta f_{ss}^{max}$	−0.5/0.5 Hz
Δt	0.1 s
$\Delta P_s^{min}/\Delta P_s^{max}$	0.01/0.15 p.u.
ΔP_{max}^{shed}	0.37 p.u.

$$K_n = \frac{1}{H_{eq}}\left(\Delta P_{n,c}^{gov} - \Delta P^{c} - D\Delta f_{n,c} + \sum_{s}^{N_s} x_{s,n,c} + \sum_{m=1}^{N_{SL}} \Delta P_{n,m}^{SL}\right) \quad (38)$$

Finally, the system frequency is determined as given in (39):

$$f_n = f_0 + f_0 * \Delta f_n \quad (39)$$

4. Scenario construction

In previous proposed UFLS plans, only a given base-case loading condition such as peak load is considered for designing UFLS, while a suitable UFLS scheme should cover different loading points under credible generation outage scenarios. In this paper, the LDC of the RTS system is utilized. In order to reduce the computational burden, the initial loading points of the RTS system are reduced to 25 loading points. These loading points are assumed to represent the most credible loading condition (i.e. peak load, medium load, and light load) of the year and vary from peak load (i.e. 1p.u.) to a base load (i.e. 0.32p.u.). Indeed, it is assumed that the LDC of the IEEE-39 bus system (see Fig. 4) has 25 loading points.

In order to analyze the low inertia condition, it is assumed that there are two wind farms at bus 34 and 37 with maximum capacities of 260 MW and 508 MW, respectively. Three levels of generation are assumed for these wind farms: (260 MW, 580 MW), (208 MW, 464 MW) and (156 MW, 348 MW). Assuming these three levels of wind generation, the penetration level of renewables at all 25 loading points results in penetration levels from 12.3% in heavy loading conditions up to 63% in base load conditions.

By considering 25 load points and 3 penetration levels for each wind farm, there will be 75 loading scenarios for the network. A UC study is carried out as formulated in [24] for each of 75 scenarios to determine the committed units in each loading condition. The total equivalent inertia of the committed units are then obtained as illustrated in Fig. 5. The UC results have been shown in Table 1.

In normal condition, the equivalent inertia based on the carried out UC studies, varies from 3.85sec to 1.7sec. Now, at each point of all 75 loading scenarios, a range of credible events are considered for UFLS scheme as given in Table 2.

The second scenario is the simultaneous double outages of generating units (i.e. N-2 outages) when the system is interconnected as a whole. The category of contingency is the islanding of power system. It is assumed that the power system is divided into isolated areas. Following the power system islanding, a possible power imbalance is expected to appear in each island. This power imbalance causes undesired frequency excursions and activates the UFLS relays. Therefore, the proposed UFLS scheme must be optimized to cover the islanding scenario too. It is assumed that the boundaries of islanding are determined using the method proposed in [25]. There is no limit to consider different islanding strategies with different boundaries as the input scenario. The last possible scenario of generation deficiency is the generation outage in each resulted islands. To this end, in this paper, the single and double outages of generating units in each island are considered as another severe generation deficiency scenario. In other words, the UFLS plan should support the frequency response under N-2 generation outages in both interconnected and islanding configurations. Finally, the scenarios given in Table 2 are considered to set the proposed UFLS plan. In other word, instead of using just one base-case scenario, the optimized UFLS plan covers more than 800 credible scenarios in the related year. It is necessary to note that topology changes after any contingencies are considered in UFLS design.

5. Simulation results

The proposed multi-stage UFLS plan is implemented on IEEE-39 bus

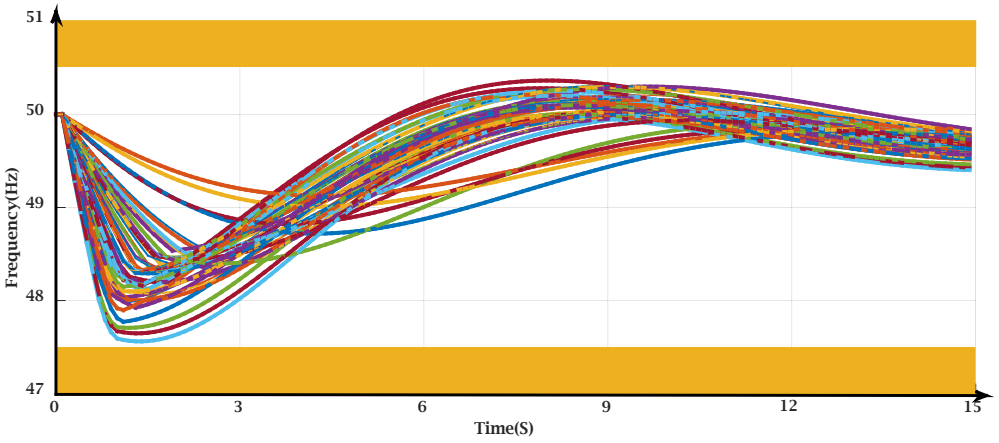

Fig. 6. Frequency responses using conventional decreasing UFLS.

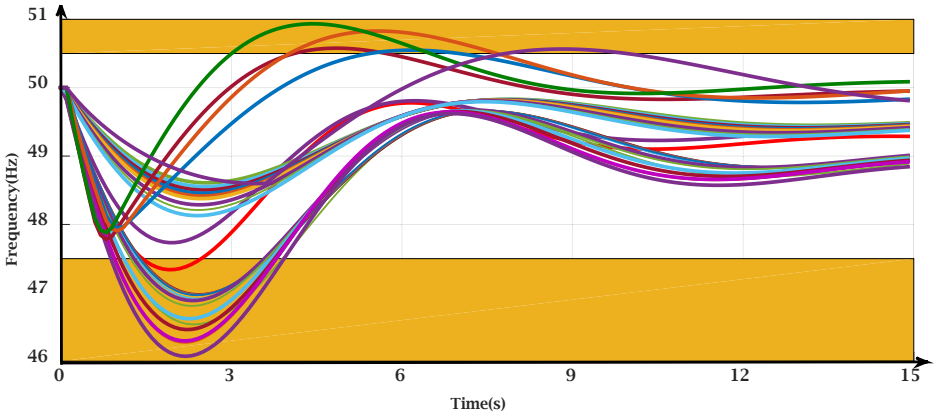

Fig. 7. Frequency responses using conventional UFLS setting in Table 4 under renewables penetration.

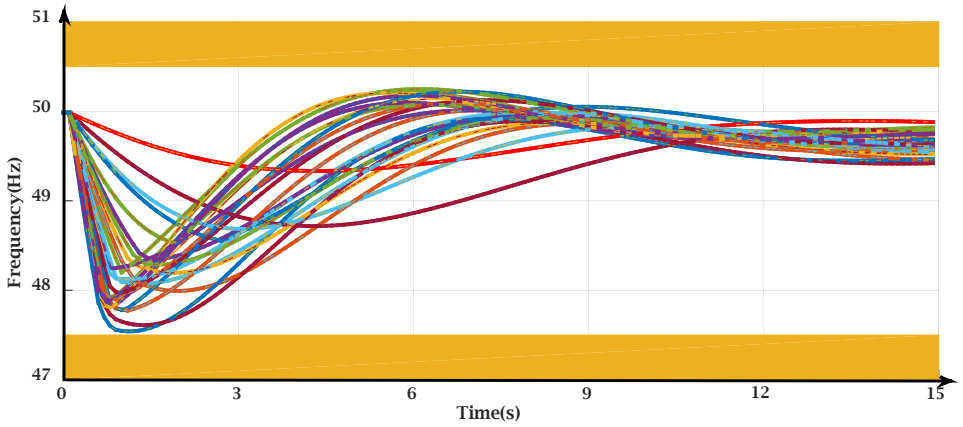

Fig. 8. Frequency responses using proposed UFLS setting in Table 4.

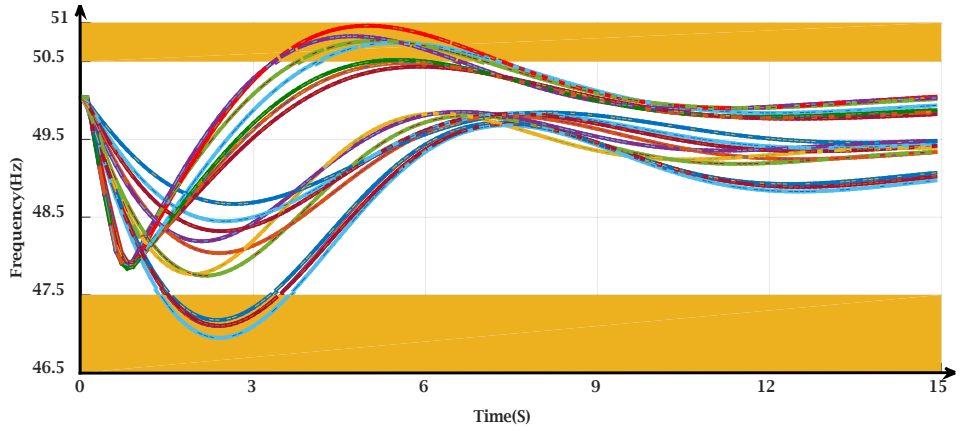

Fig. 9. Frequency responses using conventional UFLS in the presence of smart loads.

test system. The required data is reported in Table 3. More details about dynamic and static data of IEEE 39-bus test system can be found in [26]. The simulation results are presented in three different parts. In part A, the UFLS plan is optimized, conventionally, without considering renewables penetration. In part B, the performance of the conventional UFLS scheme under renewable penetration is investigated and the settings of modified UFLS plan are presented. In part C, the UFLS performance under different types of smart loads are investigated. In all three parts, the system frequency response is utilized to compare the UFLS performance. Decreasing and Increasing UFLS schemes are utilized. All MILP models are optimized using CPLEX in GAMS. In presence of renewables, the RoCoF value is utilized to adapt the UFLS system based on the actual system conditions. The ROCOF is calculated over a 500 ms time window based on the proposed method in [27]. Short time window results in unnecessary activation of UFLS plan, while the long time window incurs undesired time delay. It should be noted that the estimation of the start of an event is very important for ROCOF calculation. Some methods for anomaly detection are addressed in [28–30].

"All yellow-colored bounds in Figs. 6–11 show the forbidden area in which the network is at the risk of the cascading outages and blackout

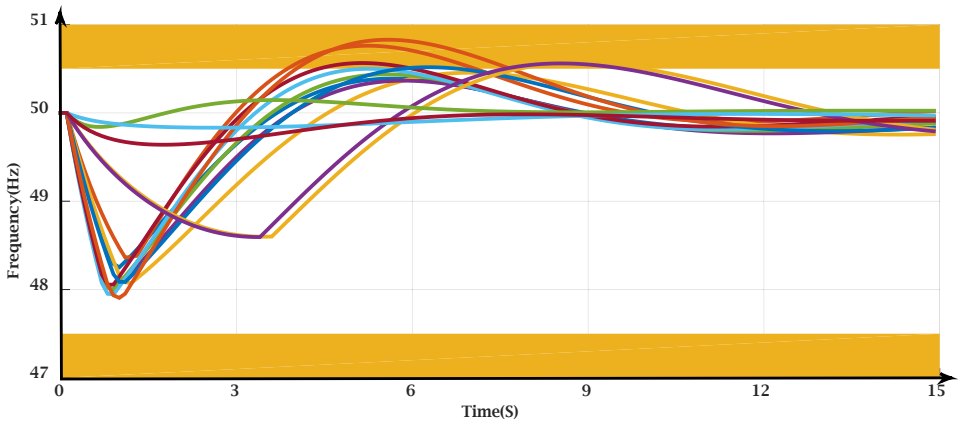

Fig. 10. Frequency responses using proposed scheme in Table 4.

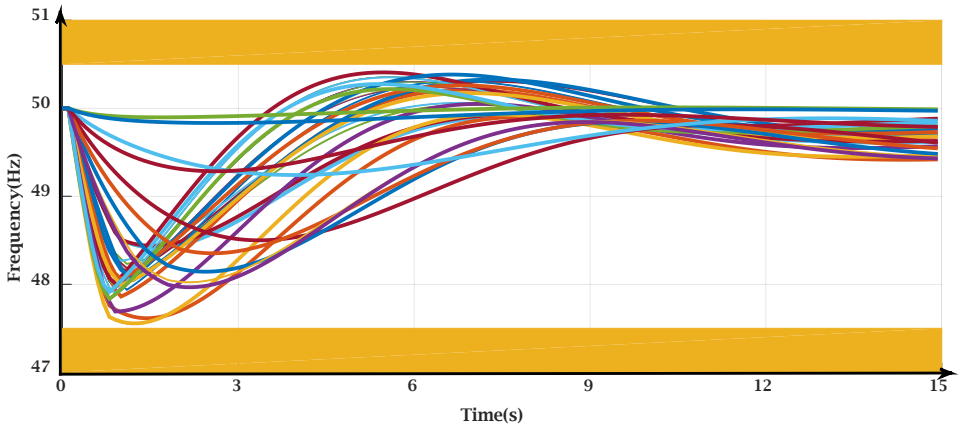

Fig. 11. Frequency responses using final UFLS setting in the presence of smart loads.

following the activation of generators circuit breaker (GCB)."

5.1. UFLS setting without considering renewable penetration

In this section, different UFLS schemes are optimized to support the frequency stability under input scenarios. Firstly, a conventional UFLS scheme is proposed without considering the wind penetration and the participation of smart loads. The optimal UFLS settings including the frequency thresholds and the amount of load shedding at each stage are reported in Table 4 and the frequency responses of the network using Decreasing UFLS method are presented in Fig. 6. It can be seen that the frequency responses under obtained settings remain in a safe range.

5.2. UFLS setting under renewable penetration scenarios

In this part, firstly, the performance of conventional settings (obtained in part A) is investigated under the renewable penetration scenarios. The system frequency responses under some operational scenarios (i.e. some selected scenarios from all input scenarios) have been depicted in Fig. 7.

It can be seen that the conventional UFLS plan fails to stabilize the frequency responses in many scenarios due to inertia deterioration. The frequency nadirs fall below 47.5 Hz which result in cascade tripping of generating units. Therefore, it is needed to optimize the UFLS setting under renewable penetration scenarios. To this end, the Decreasing UFLS scheme is optimized. The optimal settings of the Decreasing UFLS plan under renewable penetration scenarios are obtained as given in Table 4. In this scheme, based on measured RoCoF value over a 500 ms time window, two Decreasing UFLS schemes are presented. The first plan is activated if the RoCoF value is less than 1.5 Hz/s. The first UFLS plan sheds up to 10% of total loads. The second UFLS plan is activated when the RoCoF value is equal or greater than 1.5 Hz/s. By using the second plan, the UFLS relays remove up to 23.4% of network load, based on actual network loads. Fig. 8 shows the system frequency responses using the proposed semi-adaptive UFLS scheme.

In most of them, the total amount of load shedding is decreased with respect to Table 4 while all frequency responses remain in the permitted bound compared to conventional setting. It is noted that the implementation of RoCoF-based scheme is more complicated than the scheme in which the RoCoF is not considered. It should be noted that the RoCoF threshold is calculated over 500 ms time window for all scenarios. According to the simulations, half of the scenarios which are categorized as light scenarios have RoCoF less than 1.5 Hz/s and the remaining scenarios have a RoCoF greater than 1.5 Hz/s that are more sever contingencies. Additionally, it has been assumed that UFLS schemes are not activated before RoCoF measurement.

5.3. UFLS setting in the presence of smart loads

In this section, the impacts of smart loads on frequency response under the penetration of renewables is investigated. It is assumed that 10% of network total load is drive-based smart load. Further information about smart loads is presented in Table 5.

Firstly, the frequency responses are evaluated using the conventional UFLS plan (i.e. settings reported in Table 4, first column) and under the presence of smart loads. The system frequency responses are shown in Fig. 9.

As expected, the frequency nadir of scenarios are improved, but the

Table 4
Settings and Comparison of different UFLS schemes.

	UFLS settings				Proposed UFLS without smart load								Proposed UFLS with smart load							
	Conventional UFLS				Plan A				Plan B				Plan A				Plan B			
					ROCOF < 1.5 Hz/S				ROCOF≥1.5 Hz/S				ROCOF < 1.5 Hz/S				ROCOF≥1.5 Hz/S			
UFLS Stages	1^{th}	2^{th}	3^{th}	4^{th}	1^{th}	2^{th}	3^{th}	4^{th}	1^{th}	2^{th}	3^{th}	4^{th}	1^{th}	2^{th}	3^{th}	4^{th}	1^{th}	2^{th}	3^{th}	4^{th}
Frequency (Hz)	48.6	48.4	48.2	48	48.6	48.4	48.2	48	48.5	48.3	48.1	47.9	48.8	48.6	48.4	48.2	48.5	48.3	48.1	47.9
Load shedding (p.u.)	8%	6.9%	5.9%	4.7%	4%	3%	2%	1%	14.7%	3.9%	2.9%	1.9%	2.5%	3.5%	4.5%	8.7%	10.3%	4.6%	2.7%	1.7%
Some Typical Scenarios 1	✓	✓	–	–	–	–	–	–	✓	–	–	–	–	–	–	–	✓	–	–	–
2	✓	✓	✓	–	–	–	–	–	✓	✓	✓	–	–	–	–	–	✓	✓	–	–
3	✓	✓	✓	✓	–	–	–	–	✓	✓	✓	✓	–	–	–	–	✓	✓	✓	✓
4	Fails to support				–	–	–	–	✓	✓	✓	–	–	–	–	–	✓	✓	✓	✓
5	✓	✓		✓	–	–	–	–	✓	✓	✓	–	–	–	–	–	✓	✓	✓	–
6	✓	✓	✓	–	–	–	–	–	✓	✓	✓	–	–	–	–	–	✓	✓	✓	–
7	✓	✓	✓	–	–	–	–	–	✓	✓	–	–	–	–	–	–	✓	✓	–	–
8	✓	✓	✓	✓	–	–	–	–	✓	✓	✓	✓	–	–	–	–	✓	✓	✓	–
9	Fails to support				–	–	–	–	✓	✓	✓	–	–	–	–	–	✓	✓	✓	–
10	Fails to support				–	–	–	–	✓	✓	✓	–	–	–	–	–	✓	✓	✓	–
11	✓	–	–	–	✓	✓		–	–	–	–	–	✓	–	–	–	–	–	–	–
12	✓	✓	–	–	✓	✓	✓	–	–	–	–	–	✓	✓	–	–	–	–	–	–
13	✓	–	–	–	✓	✓		–	–	–	–	–	✓	✓	–	–	–	–	–	–
14	✓	✓	–	–	✓	✓	✓	✓	–	–	–	–	✓	✓	–	–	–	–	–	–
Total Shedding (p.u.) for above scenarios	2.808				2.44								1.872							

Table 5
Parameters of utilized dynamic smart loads.

Type	Percentage of total smart load	*kpf*	$*f^{dr-min}$	T_s	Application
Space heating	35%	2.64	43 Hz	0.5 s	HVAC systems, Coolers
Large industrial motor	21%	2.97	40 Hz	0.6 s	Massive compressors and industrial equipment
Small industrial motor	26%	2.95	40 Hz	0.4 s	Conveyor lines, pumps
Compressed air	18%	2.99	42 Hz	0.7 s	Rock drilling, chemical industry, metallurgy

* Minimum allowable operating drive frequency of smart loads

frequency overshoot and frequency nadir still violates the allowed limitation. Secondly, the system frequency responses are depicted in Fig. 10 using the UFLS plan (i.e. the settings reported in Table 4, second column), and under the presence of smart loads. Although, in this case, the UFLS plan gives better results with respect to the conventional UFLS, but, in some scenarios it causes undesired overshoots in frequency responses. Moreover, it sheds more load according to Table 4.

Regarding these issues, the proposed UFLS scheme should be re-optimized to avoid overshoot in frequency response and unnecessary load shedding. Therefore, a new UFLS scheme is obtained as given in Table 4 (third column) which considers high penetration of renewable resources (i.e. 63%), with 10% smart load. Plan A is an Increasing UFLS design and is activated under moderate outages with a ROCOF less than 1.5 Hz/s. Plan B is a Decreasing UFLS design that is activated for the generation outages with a RoCoF equal or greater than 1.5 Hz/s. The main merit of the proposed method is that the amount of load shedding using the proposed method is reduced, significantly. According to Fig. 11, the frequency responses are stabilized without any undesired frequency nadir or frequency overshoot.

According to the proposed model for smart loads, they reduce their consumptions rapidly and enters into a saturation phase. By deploying the spinning reserves of conventional units, the smart loads backs to their normal consumption as shown in Fig. 12.

To compare the proposed UFLS schemes, Table 4 gives the performance of each UFLS scheme under 14 selected scenarios from all scenarios, indicating activated load shedding stages. It can be deduced that both schemes (i.e. the scheme under renewable penetration, and the scheme under renewable penetration and smart loads) are considerably better than conventional UFLS designs. However, the UFLS scheme using smart loads, not only covers all the scenarios, but also impressively has reduced the amount of required load shed. Therefore, it is the most suitable setting for the network. The expression "Fails to support" which has been written for fourth, 9th and 10th scenario in conventional UFLS setting, means that, conventional UFLS setting under low inertia conditions cannot keep the frequency of the network in allowed bound. On the other word, using this setting, frequency inters into the yellow-colored bound area or even below the yellow bound as shown in Fig. 7.

Briefly, the whole structure and performance logic of the proposed method from the UFLS relays point of view is shown in flowchart Fig. 13.

5.4. Uncertainty of smart loads

In this section, the effect of smart loads participation on UFLS design is investigated. According to Table 6, It can be seen that by increasing the share of smart load, the total required load shedding by UFLS scheme is decreased. Another important issue is that the operating frequency of smart loads is an uncertain variable, and as a result, the amount of smart load reserve or contribution in frequency support is not known

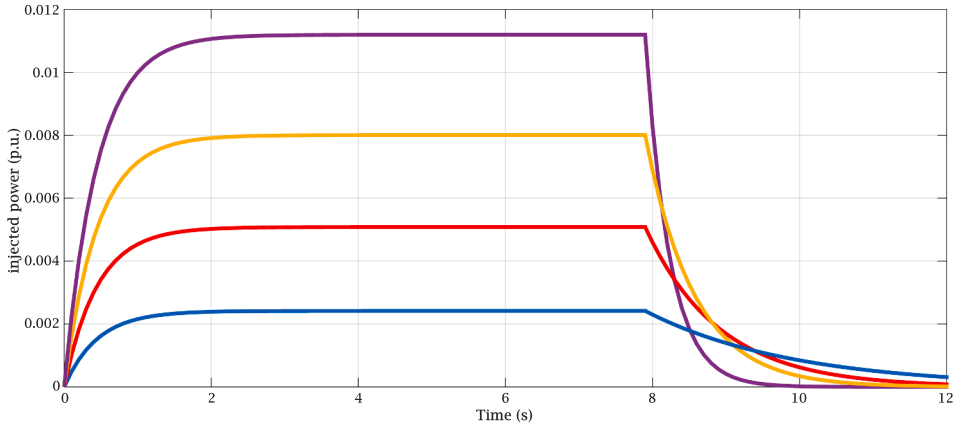

Fig. 12. Dynamic response of the smart loads.

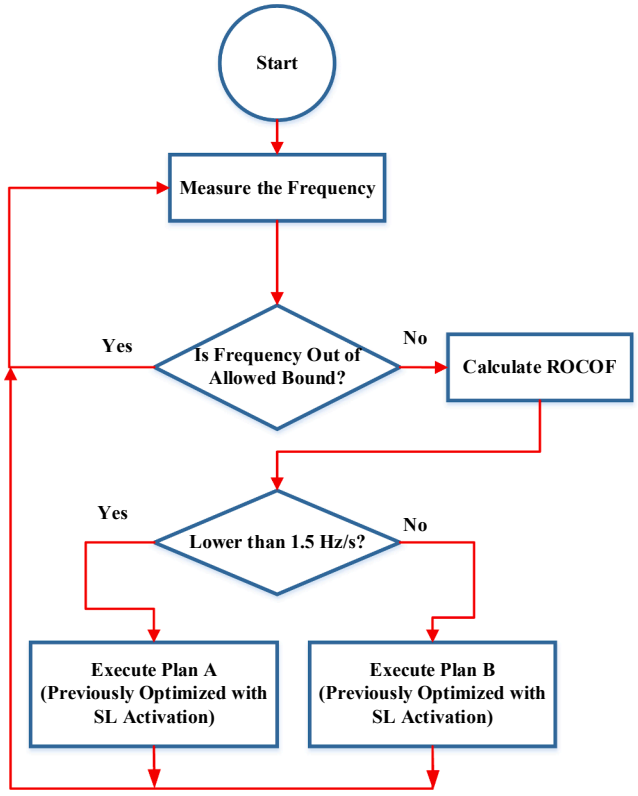

Fig. 13. Flowchart of the proposed method from the relays point of view.

Table 6
UFLS setting under different shares of smart loads.

SL (%)*	Stage1	Stage2	Stage3	Stage4	Total
0%	48.5	48.3	48.1	47.9	23.4%
	14.7%	3.9%	2.9%	1.9%	
5%	48.4	48.2	48	47.8	21.5%
	14.6%	3.3%	2.3%	1.3%	
10%	48.5	48.3	48.1	47.9	19.3%
	10.3%	4.6%	2.7%	1.7%	
15%	48.5	48.3	48.1	47.9	17.1%
	7%	5.1%	3%	2%	
20%	48.4	48.2	48	47.8	15.2%
	5.8%	4.8%	2.9%	1.7%	

* Smart load participation

deterministically. Therefore, an uncertainty study based on Monte-Carlo simulation is done to show the expected performance of UFLS under smart load contribution. Fig. 14 shows the normal random distribution of drive operating frequency of smart loads in which the mean and deviation of smart loads are assumed to be (48 Hz, 1.3 Hz), (48.5 Hz, 1.2 Hz), (47.5 Hz, 1.1 Hz), and (47.5 Hz, 1.05 Hz), respectively. Fig. 15 shows the distribution of resulted nadir frequencies in a generation outage as $\Delta P^{c} = 0.25$p.u. with$H_{eq} = 2.2$s, using 1600 samples of smart load operating frequency based on Monte-Carlo simulation. Fig. 12 shows under different participations of smart loads, frequency nadir has normal distribution between 48.06 Hz and 48.17 Hz with the mean of 48.11 Hz.

6. Conclusion

In this paper, a novel UFLS scheme was presented. Unlike previous proposed UFLS plans that only set the UFLS at peak load, this paper considers credible loading points according to annual LDC. Moreover a wide range of wind penetration scenarios along with smart load participation have been taken into account. The major findings of this paper are summarized as follows:

1) The high penetration of non-synchronous renewable resources affects the network inertial response and UFLS setting under severe generation outages.
2) The conventional multistage UFLS plan optimized without considering renewable penetrations fail to restore the system frequency under generation deficiency.
3) The UFLS setting considering only the peak load conditions, is not realistic and results in undesired system frequency responses under credible operating points in a given year.
4) Under high penetration of non-synchronous renewable resources, the inertial response is strongly sharp, requiring Decreasing UFLS scheme to enhance the system frequency support.
5) The participation of smart loads, especially industrial motors equipped with drive system has a significantly positive impact on frequency support. In the presence of smart loads the frequency nadir will be improved while the amount of load shedding is reduced. By postponing the UFLS activation, low inertia networks by using smart loads will be more flexible against different unpredictable contingencies.

CRediT authorship contribution statement

A. Darbandsari: Conceptualization, Methodology, Software, Writing – original draft. **T. Amraee:** Conceptualization, Supervision, Methodology, Validation, Writing – review & editing.

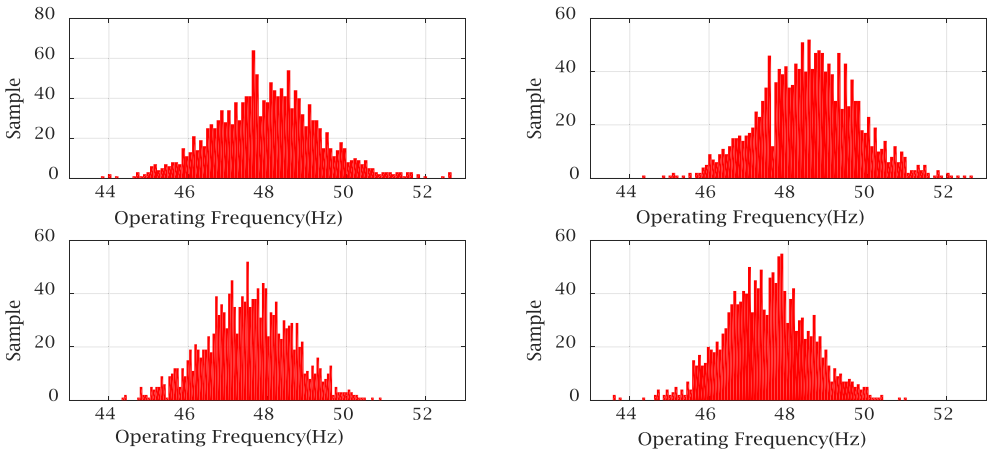

Fig. 14. PDFs of input operating frequency of smart loads.

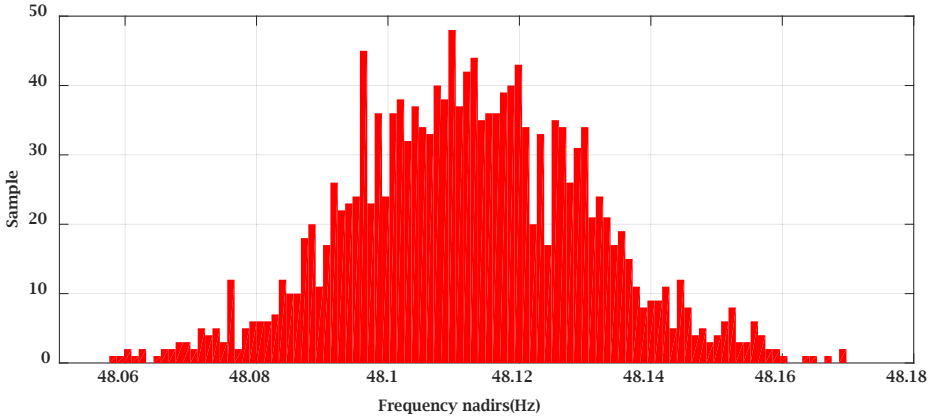

Fig. 15. PDF of the resulted frequency nadirs.

Declaration of Competing Interest

The authors declare that they have no known competing financial interests or personal relationships that could have appeared to influence the work reported in this paper.

References

[1] Gevorgian V, Zhang Y, Ela E. Investigating the impacts of wind generation participation in interconnection frequency response. IEEE Trans Sustainable Energy 2015;6(3):1004–12.
[2] Gu H, Yan R, Saha TK. Minimum synchronous inertia requirement of renewable power systems. IEEE Trans Power Syst 2018;33(2):1533–43.
[3] [Online]: https://www.nationalgrideso.com/information-about-great-britains-energy-system-and-electricity-system-operator-eso [access: 3 Jan 2020].
[4] Das K, Nitsas A, Altin M, Hansen AD, Sorensen PE. Improved load-shedding scheme considering distributed generation. IEEE Trans Power Delivery 2017;32(1):515–24.
[5] Ghaderi Darebaghi M, Amraee T. Dynamic multi-stage under frequency load shedding considering uncertainty of generation loss. IET Gener Transm Distrib 2017;11(13):3202–9.
[6] POWER SYSTEMS RELAYING COMMITTEE, et al. IEEE Guide for the Application of Protective Relays Used for Abnormal Frequency Load Shedding and Restoration. IEEE Std C, 2007, 37: c1-c43.
[7] Amraee Turaj, Darebaghi Mohammad Ghaderi, Soroudi Alireza, Keane Andrew. Probabilistic under frequency load shedding considering rocof relays of distributed generators. IEEE Trans Power Syst 2018;33(4):3587–98.
[8] Banijamali Seyed Sohrab, Amraee Turaj. Semi adaptive setting of under frequency load shedding relays considering credible generation outage scenarios. IEEE Trans Power Delivery 2019;34(3):1098–108.
[9] Rudez Urban, Mihalic Rafael. WAMS-based underfrequency load shedding with short-term frequency prediction. IEEE Trans Power Delivery 2016;31(4):1912–20.
[10] Shekari Tohid, Aminifar Farrokh, Sanaye-Pasand Majid. An analytical adaptive load shedding scheme against severe combinational disturbances. IEEE Trans Power Syst 2016;31(5):4135–43.
[11] Hong Ying-Yi, Chen Po-Hsuang. Genetic-based underfrequency load shedding in a stand-alone power system considering fuzzy loads. IEEE Trans Power Delivery 2012;27(1):87–95.
[12] Hong Ying-Yi, Hsiao Ming-Chun, Chang Yung-Ruei, Lee Yih-Der, Huang Hui-Chun. Multiscenario underfrequency load shedding in a microgrid consisting of intermittent renewables. IEEE Trans Power Delivery 2013;28(3):1610–7.
[13] Issicaba Diego, da Rosa Mauro Augusto, Resende Fernanda Oliveira, Santos Bruno, Peças Lopes João Abel. Long-term impact evaluation of advanced under frequency load shedding schemes on distribution systems with DG islanded operation. IEEE Trans Smart Grid 2017;10(1):238–47.
[14] Hong Ying-Yi, Nguyen Manh-Tuan. Multiobjective multiscenario under-frequency load shedding in a standalone power system. IEEE Syst J 2020;14(2):2759–69.
[15] Li Changgang, Wu Yue, Sun Yanli, Zhang Hengxu, Liu Yutian, Liu Yilu, et al. Continuous under-frequency load shedding scheme for power system adaptive frequency control. IEEE Trans Power Syst 2020;35(2):950–61.
[16] Ochoa Danny, Martinez Sergio. Fast-frequency response provided by DFIG-wind turbines and its impact on the grid. IEEE Trans Power Syst 2017;32(5):4002–11.
[17] Delille Gauthier, Francois Bruno, Malarange Gilles. Dynamic frequency control support by energy storage to reduce the impact of wind and solar generation on isolated power system's inertia. IEEE Trans Sustainable Energy 2012;3(4):931–9.
[18] Lai Chao-Yuan, Liu Chih-Wen. A scheme to mitigate generation trip events by ancillary services considering minimal actions of UFLS. IEEE Trans Power Syst 2020;35(6):4815–23.
[19] Chakravorty Diptargha, Chaudhuri Balarko, Hui Shu Yuen Ron. Rapid frequency response from smart loads in great britain power system. IEEE Trans Smart Grid 2017;8(5):2160–9.
[20] Wang Jidong, Zhang Huiying, Zhou Yue. Intelligent under frequency and under voltage load shedding method based on the active participation of smart appliances. IEEE Trans Smart Grid 2017;8(1):353–61.
[21] Drabandsari Amir, Amraee Turaj. Optimal setting of under frequency load shedding relays in low inertia networks. In: 2018 Smart Grid Conference (SGC). IEEE; 2018. p. 1–6.
[22] Kwak ByungGil, Um Jeong-Heum, Seok Jul-Ki. Direct active and reactive power control of three-phase inverter for AC motor drives with small DC-link capacitors fed by single-phase diode rectifier. IEEE Trans Ind Appl 2019;55(4):3842–50.

[23] Javadi Masoud, Amraee Turaj, Capitanescu Florin. Look ahead dynamic security-constrained economic dispatch considering frequency stability and smart loads. Int J Electr Power Energy Syst 2019;108:240–51.
[24] Naghdalian Salar, Amraee Turaj, Kamali Sadegh. Linear daily UC model to improve the transient stability of power system. IET Gener Transm Distrib 2019;13(13):2877–88.
[25] Teymouri Farhad, Amraee Turaj. An MILP formulation for controlled islanding coordinated with under frequency load shedding plan. Electr Power Syst Res 2019;171:116–26.
[26] [Online];https://www.kios.ucy.ac.cy/testsystems/index.php/dynamic-ieee-test-systems/ieee-39-bus-modified-test-system [Access: 5 Jan 2020].
[27] Frigo Guglielmo, Derviskadic Asja, Zuo Yihui, Paolone Mario. PMU-based ROCOF measurements: Uncertainty limits and metrological significance in power system applications. IEEE Trans Instrum Meas 2019;68(10):3810–22.
[28] Kovalenko Pavel Y, Berdin Alexander S, Bliznyuk Dmitry I, Plesnyaev Evgeny A. The flexible algorithm for identifying a disturbance and transient duration in power systems. In: 2016 International Symposium on Industrial Electronics (INDEL); 2016. p. 1–4.
[29] Dai Hua, Sun Xin, Li Jiyuan, Zhang Guoming, Ji Xiaoyu, Xu Wenyuan. Power consumption-based anomaly detection for relay protection. In: 2020 IEEE 4th information technology, networking, electronic and automation control conference (ITNEC), vol. 1. IEEE; 2020. p. 1139–43.
[30] Wang Zhongfeng, Fu Yatong, Song Chunhe, Zeng Peng, Qiao Lin. Power system anomaly detection based on OCSVM optimized by improved particle swarm optimization. IEEE Access 2019;7:181580–8.